

Article

A Novel Laser-Aided Machining and Polishing Process for Additive Manufacturing Materials with Multiple Endmill Emulating Scan Patterns

Mohammad Masud Parvez ^{*,†} , Sahil Patel, Sriram Praneeth Isanaka and Frank Liou 

Department of Mechanical and Aerospace Engineering, Missouri University of Science and Technology, Rolla, MO 65401, USA; sbpbg8@umsystem.edu (S.P.); sihyd@umsystem.edu (S.P.I.); liou@umsystem.edu (F.L.)

* Correspondence: mphf2@umsystem.edu; Tel.: +1-573-202-1506

† Current address: 200 Monterey Street, Brisbane, CA 94005, USA.

Abstract: In additive manufacturing (AM), the surface roughness of the deposited parts remains significantly higher than the admissible range for most applications. Additionally, the surface topography of AM parts exhibits waviness profiles between tracks and layers. Therefore, post-processing is indispensable to improve surface quality. Laser-aided machining and polishing can be effective surface improvement processes that can be used due to their availability as the primary energy sources in many metal AM processes. While the initial roughness and waviness of the surface of most AM parts are very high, to achieve dimensional accuracy and minimize roughness, a high input energy density is required during machining and polishing processes although such high energy density may induce process defects and escalate the phenomenon of wavelength asperities. In this paper, we propose a systematic approach to eliminate waviness and reduce surface roughness with the combination of laser-aided machining, macro-polishing, and micro-polishing processes. While machining reduces the initial waviness, low energy density during polishing can minimize this further. The average roughness ($R_a = 1.11 \mu\text{m}$) achieved in this study with optimized process parameters for both machining and polishing demonstrates a greater than 97% reduction in roughness when compared to the as-built part.

Keywords: additive manufacturing; direct energy deposition; aluminum deposition; laser-aided machining; macro-polishing; micro-polishing



Citation: Parvez, M.M.; Patel, S.; Isanaka, S.P.; Liou, F. A Novel Laser-Aided Machining and Polishing Process for Additive Manufacturing Materials with Multiple Endmill Emulating Scan Patterns. *Appl. Sci.* **2021**, *11*, 9428. <https://doi.org/10.3390/app11209428>

Academic Editors: Volker Wesling and Kai Treutler

Received: 20 September 2021

Accepted: 8 October 2021

Published: 11 October 2021

Publisher's Note: MDPI stays neutral with regard to jurisdictional claims in published maps and institutional affiliations.



Copyright: © 2021 by the authors. Licensee MDPI, Basel, Switzerland. This article is an open access article distributed under the terms and conditions of the Creative Commons Attribution (CC BY) license (<https://creativecommons.org/licenses/by/4.0/>).

1. Introduction

Additive manufacturing (AM) is an emerging manufacturing process applied both in research and industrial fields such as aerospace, biomedical, space, defense, naval, energy sectors, automotive, oil and gas industries, and others [1–3]. This process can be used for the production of parts with complex geometries that are otherwise difficult to produce using conventional manufacturing processes [4–6]. The complex, lightweight, and customized parts manufactured by the AM process can significantly minimize the consumption of raw materials and improve the competence in real field application. Therefore, AM is increasingly being used in different manufacturing fields. While AM has several advantages over conventional manufacturing processes, parts produced with this process exhibit poor surface roughness and geometric inaccuracy in their as-built state [7–10]. Several studies have recently been carried out to investigate the factors for dimensional inaccuracy and poor surface quality of metal AM parts. Surface tension associated with temperature gradients of the melt pool can cause rapid hydrodynamic motions known as Marangoni flow, resulting in dishing or humping [11,12]. Balling of material caused by long thin melt pools degrades surface roughness [13–15]. Another process phenomenon degrading the surface quality of AM parts is the staircase effect, which is the result of layer-wise approximation of part geometry [16]. Fabrication process parameters also influence the

surface roughness. High energy density helps in reducing top and side surface roughness while repetitive laser melting and slow scan speed increase side surface roughness but decrease top surface roughness [17,18]. Partially fused powder particles are also a common cause of high surface roughness in AM parts [19]. Due to all the factors mentioned above, achieving admissible ranges of surface roughness and geometric dimension and tolerance (GD&T) is very difficult in the AM process. Therefore, post-processing, especially surface treatment, is required to qualify AM parts for final applications.

In most applications, especially for usages critical to fatigue [20], post-fabrication surface treatments such as machining, grinding, and polishing are preferred for AM metal parts. Conventional machining and polishing processes are usually employed to improve the part surface finish and bring it within GD&T. Spierings et al. [21] utilized a CNC lathe to finish AISI 316 and 15-5 HP steel parts built with AM techniques and improved the fatigue performance of the parts. Taminger et al. [22] applied high-speed milling (HSM) to finish AM aluminum parts and evaluated the effectiveness of the different surface finishing techniques to achieve a smooth surface finish. Löber et al. [23] reduced the as-built surface roughness of AISI 316L steel parts using different surface treatment processes such as grinding, sandblasting, and electrolytic and plasma polishing. They also compared and quantified the change in surface roughness after different surface treatments. Beauchamp et al. [24] introduced a novel shape-adaptive grinding process to finish AM Ti6Al4V parts and smoothed down the surface to less than 10 nm average roughness from 4 to 5 μm . Flynn et al. [25] implemented a hybrid manufacturing system by combining additive and subtractive methods to mitigate surface roughness.

Besides conventional surface quality improvement processes, laser-aided machining and polishing (LAMP) can also be an effective method to achieve dimensional accuracy and minimize roughness [26–30]. LAMP offers a high processing rate, minimum heat-affected zone (HAZ), and easily adjustable process parameters [31,32]. This method can also repair cracks and pores, ablate metallic globules, and improve the fatigue performance of AM materials [33,34]. The LAMP technique is also advantageous over commonly used processes since the size of the tools used in conventional methods for machining and polishing has limitations to reach critical locations. Additionally, while a hybrid manufacturing process combined with the AM system makes the entire process unwieldy and complicated, LAMP can be easily integrated with any existing laser-enabled AM process. Among different AM techniques available, i.e., selective laser melting (SLM), electron beam melting (EBM), powder fed and wire fed direct energy deposition (DED), laser-aided SLM and DED processes are very popular methods used to fabricate ferrous and nonferrous materials. Toward improving the surface finish and obtaining GD&T for AM parts, by utilizing the same laser employed to fabricate AM parts, surface roughness can be improved in the same build chamber or machine.

Toward modeling and developing the LAMP process and investigating the effect of this process on the mechanical properties of AM materials, several studies have recently been carried out [35–46]. Chow et al. [47] demonstrated the application of pulsed laser (PL) for both micro-milling and micro-polishing processes by changing the focal offset distance between the laser focus and the part surface. Perry et al. [48] investigated the effect of laser pulse duration and feed rate variation on surface polishing. Ramos et al. [49] studied the effect of shallow surface melting and surface over melting on the laser polishing process. Schneider et al. [50] discussed the general properties of PL machining relevant to solid-state physics such as the initial ablation process and the formation and properties of the plume. Brown et al. [51] performed a fundamental study on laser metal interaction and its application to surface modification without altering the part geometry. Marimuthu et al. [32] developed a numerical model based on a computational fluid dynamic formulation to understand the melt pool dynamics during laser polishing. They identified the input thermal energy as the key parameter affecting melt pool convection and controlling the surface quality. Rosa et al. [52] proposed a quadratic model taking into account the initial surface topography and polishing process parameters. Using the model, they predicted

the polished surface quality and also experimentally determined the optimal parameters for polishing. Chen et al. [53] investigated the formation of bulge structure during laser polishing and the influence of processing parameters on the bulge structure through parametric analyses. Yung et al. [54] made use of PL to polish complex geometries, i.e., convex, concave, and slant geometries made of AM CoCr alloy, and achieved a 93% reduction in surface roughness with an 8% hardness enhancement.

While PL has been reported to be applied mostly for LAMP, several researchers have also employed continuous wave (CW) lasers alone or combined with PL and demonstrated improvements in surface roughness [40,55,56]. Solheid et al. [57] investigated the effect of using CW laser and PL on improving the surface roughness of AM 18Ni (300 grade) Maraging steel. A stable melt pool with fine surface finishing was observed for PL polishing at low power and low speed, while a significant improvement in surface quality was achieved with CW laser at high scan speed and laser power. By utilizing both CW laser and PL together, Nüsser et al. [58] deployed a dual-beam technology for surface polishing. CW laser was used for preheating the surface and PL polished the preheated surface. The dual-beam polishing process demonstrated a higher reduction in surface roughness in comparison to the conventional laser polishing process. Caggiano et al. [59] introduced an innovative laser polishing process implementing a wobble amplitude pattern during polishing and applied a convolutional neural network (CNN)-based artificial intelligence technique on polished surface images to identify optimal process parameters for polishing.

In previous studies, while different techniques and methods have been presented using both CW laser and/or PL for the laser-aided polishing process [26–30,47,48,59], further investigation is required to develop a comprehensive and combined process while selecting the scan patterns and types of lasers for machining and polishing AM materials using lasers. In this study, we propose a unique laser-aided machining and polishing (LAMP) process with the combination of CW laser, pulsed laser, and a novel scan pattern that emulates end mills of different sizes while machining and fine polishing the material. For the LAMP process, the Scalmalloy aluminum alloy was fabricated using the DED process and the process parameters were optimized in each step of machining (micro-milling) and polishing (macro-polishing and micro-polishing) to reduce the surface roughness and improve the surface quality of the material.

2. Materials and Methods

2.1. Materials

The material used in this study was Ar gas atomized aluminum alloy powder referred to as Scalmalloy purchased from APWORKS GmbH (Taufkirchen, Germany). The powder was sieved to a particle size of 105 µm for the powder-fed DED process. Scalmalloy is a high-strength lightweight alloy widely used in the AM process for aluminum deposition [60–62]. The material also exhibits excellent corrosion resistance. Because of its wide range of applications in robotics, aerospace, marine, and automotive industries, the material was chosen in this study. The chemical composition of the material is presented in Table 1.

Table 1. Chemical composition of Scalmalloy powder particles in weight percentage (wt%).

Element	Al	Mg	Sc	Zr	Mn	Si	Fe	Zn	Cu	Ti	O	V
wt.%	bal.	4.00–4.90	0.60–0.80	0.20–0.50	0.30–0.80	<0.40	<0.40	<0.25	<0.10	<0.15	<0.05	<0.05

2.2. Methodology

2.2.1. Experimental Setup

The LAMP technique is advantageous over conventional machining and polishing processes because of the flexibility of integration with any existing laser-enabled AM process. Additionally, the laser used for material deposition can also be employed for the LAMP process. Figure 1 shows the experimental setup designed and developed for this study. The LAMP system integrated with a powder-fed DED process consists of a

stepper motor-driven gantry, a CW high-power (2 KW) laser, a low-power (100 W) PL, a galvanometer, an F-theta scan lens, and a servo-controlled powder feeder. In this study, material deposition and macro-polishing were carried out with CW laser while PL was used for machining and micro-polishing processes. The CW laser was focused using a 200 mm focal length focusing optic. A 2-Axis scanning galvanometer (GVS312) from Thorlabs combined with a FTH254 F-Theta scanning lens was used for PL scanning. The effective focal length of the F-Theta lens was 254 mm. A two-channel arbitrary signal generator (SDG2042X) from SIGLENT Technologies North America, Inc. (Solon, OH, USA) was used to generate a true waveform shape for PL scanning. The powder was fed using an X2W powder feeder from Powder Motions Labs (Rolla, MO, USA) and focused on using an in-house custom-designed nozzle with a ceramic tube. The standoff distance between the workpiece and the nozzle was kept at 12.5 mm for effective powder catchment. Argon gas was supplied as the shielding gas for the environment and the CW laser and carrier gas for the powder supply. All the hardware and peripherals were connected together with a LinuxCNC operating system to develop the hybrid manufacturing system integrated for AM and LAMP processes.

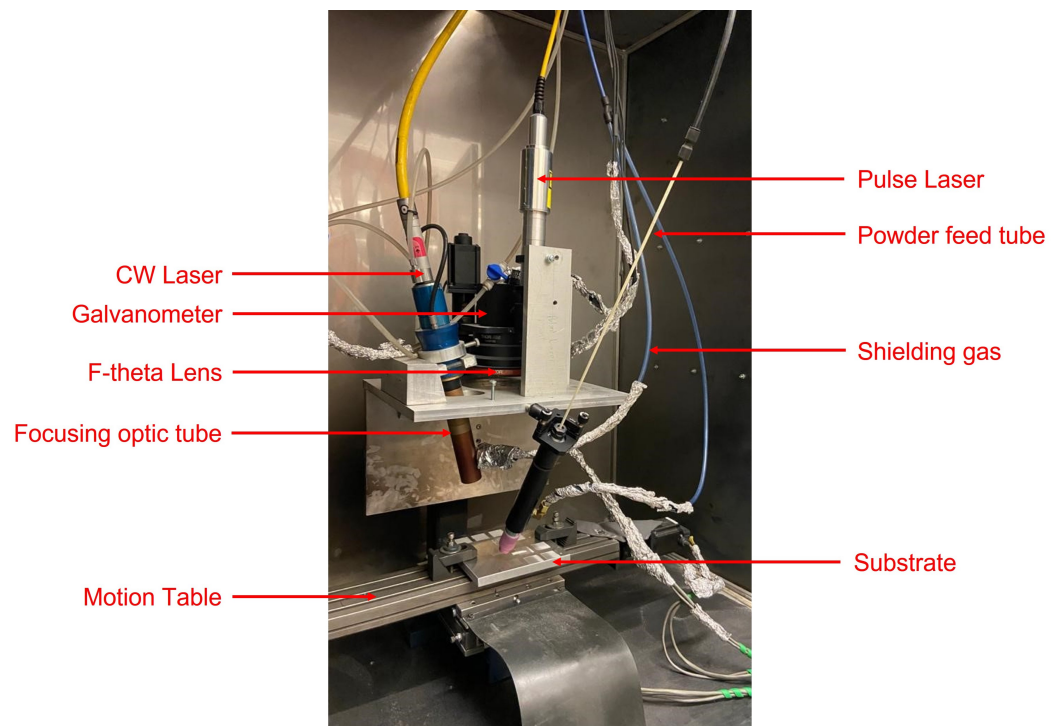


Figure 1. Experimental setup used in this study for direct energy deposition (DED) and laser-aided machining and polishing (LAMP) processes.

2.2.2. Fabrication

Aluminum is a highly reflective and thermally conductive material for any laser-enabled AM process. Therefore, a high-power TeraBlade-2000 direct-diode 949–1001 nm wavelength CW laser (TeraDiode, a Panasonic company, Wilmington, MA, USA) was used in this study to fabricate Scalmalloy. Laser-enabled AM processes can be classified into three categories such as powder-bed SLM, powder-fed DED, and wire-fed DED. In all these processes, the surface exhibits a waviness profile and roughness. The surface roughness and waviness are defined by ASME B46.1 [31,63] as low-frequency and high-frequency components, respectively. The surface roughness depends on the input energy density applied to fabricate the material. Poor energy density choices during deposition yield material defects that mimic bulge-like structures on the surface and increase the surface roughness [53] while high-wavelength surface features (waviness) exist on the surface of AM parts because of the layer width and thickness. These features are especially high

in the DED process, where the beam size is larger compared to the SLM process beam size, and the track overlap leads to a wavy surface pattern. Therefore, in this study, the powder-fed DED process was employed with no raster rotation to obtain an initially high surface roughness after deposition. Figure 2a exhibits the schematic representation of the raster pattern used for material deposition. The fabrication process parameters used to deposit Scalmalloy are listed in Table 2. Based on the design of experiments, a total of 44 rectangular patches with dimensions of 27 mm × 27 mm × 1 mm were deposited to obtain optimized LAMP process parameters for good surface quality. All the samples were deposited on 5000 series aluminum alloy substrate (152.4 mm × 152.4 mm × 12.7 mm). Among 44 rectangular deposits, 12 samples were used for the machining process while half of the remaining samples were used for macro-polishing and the rest for the micro-polishing process. Figure 3a shows the first 12 samples deposited and used for optimizing the machining process.

Table 2. Fabrication process parameters used to deposit Scalmalloy.

Parameters	Laser Power (W)	Travel Speed (mm/min)	Layer Width (mm)	Layer Thickness (mm)	Overlap Between Tracks (%)	Raster Rotation (degree)	Powder Flow Rate (g/min)	Shield Gas Flow Rate (L/min)
Value	1600	500	2.5	0.300	30	0	6	4

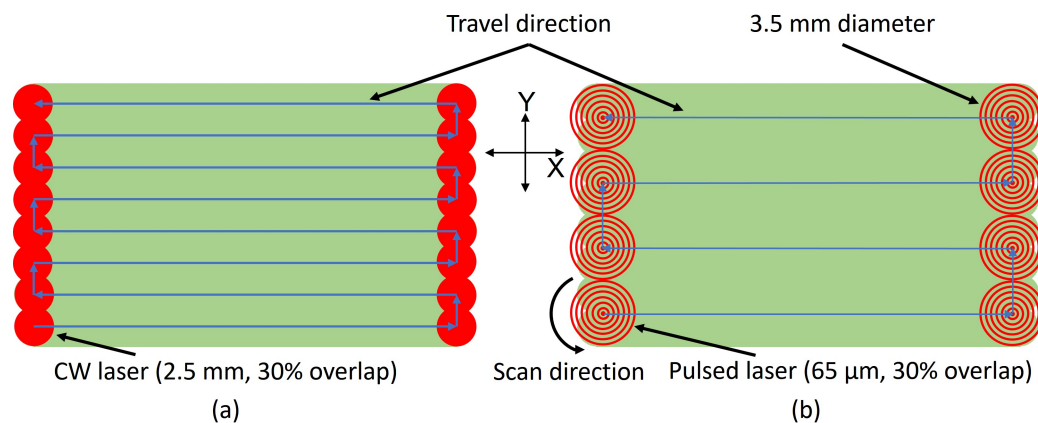


Figure 2. Schematic representation (not to scale) of (a) the CW laser scan pattern for material deposition and macro-polishing and (b) pulsed laser scan pattern for machining and micro-polishing. The PL scan pattern rotates radially inward in an anti-clockwise direction.

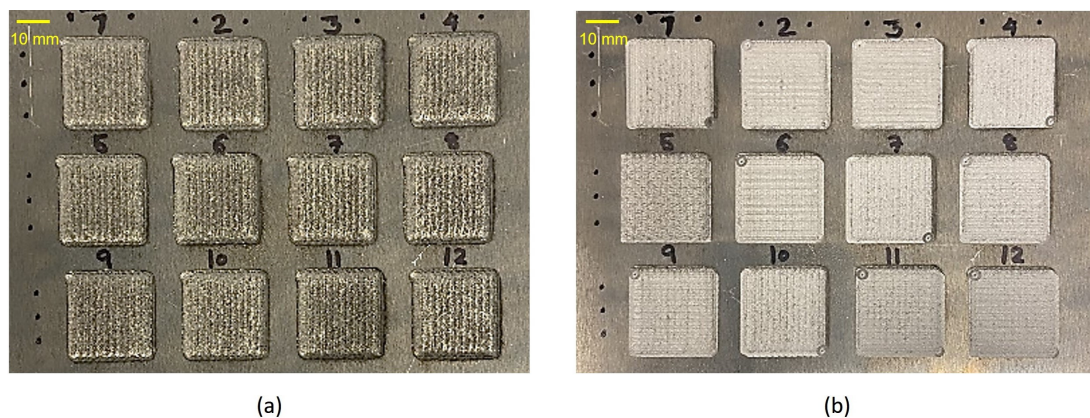


Figure 3. Top view of Scalmalloy samples from #1 to #12 (a) deposited with process parameters mentioned in Table 2 and (b) machined with different process parameters presented in Table 3.

2.2.3. Machining

In the laser-aided polishing process, the top surface of an AM part is remelted and the material is redistributed from peaks of the surface to the valleys because of surface tension and gravity [64,65]. However, laser polishing alone cannot remove certain surface features with high wavelengths. A machining process before polishing can help to minimize high-wavelength surface waviness. In order to ablate materials, the laser machining process may require high input energy, but higher input energy can originate additional wavy features because of the mass transport of the fluid flow in the melting pool. Therefore, we proposed a unique laser-enabled machining process that utilizes low input energy density to ablate materials. In this study, we introduced a novel PL scan pattern. Figure 2b shows the schematic representation of the scan pattern and its travel direction used during machining cycles. The overall diameter of the scan pattern was set at 3.5 mm, which is twice the layer width including hatch spacing during material deposition. This pattern is a modified version of the wobbling scan pattern introduced by Caggiano et al. [59]. The unique feature of this pattern is that while machining the top surface of the deposited samples, the pattern emulates end mills of multiple sizes commonly used in the CNC milling process. In such a way, these patterns offer a high processing rate with low thermal energy input during machining. The number of laser scanning passes on the top surface of the material depends on the scan speed, travel speed, total diameter of the scan, laser spot size, and the sum of the circumference of the scan pattern. Equation (1) was derived to calculate the number of passes per mm during PL scanning.

$$PPM = \frac{S_S}{S_T} \times \frac{2 \times N_C}{L_S} \quad (1)$$

where S_S , S_T , PPM , N_C , and L_S are the scan speed, travel speed, number of laser scan passes per mm, number of circles in the scan pattern, and total length of PL scans in the pattern, respectively. The scan length is the sum of the circumference circles in a scan pattern given by Equation (2),

$$L_S = 2 \times \pi \times \sum_{i=0}^{N_C-1} (R - i \times r \times (1 - O_p)) \quad (2)$$

where R and r are the radius of the scan pattern and laser spot size, respectively. O_p is the overlap. The number of circles in the scan pattern can be calculated using Equation (3).

$$N_C = \frac{R}{r \times (1 - O_p)} \quad (3)$$

In this study, a 100 W PL (YLP-V2, IPG Photonics, Oxford, MA, USA) with 1055–1075 nm wavelength, 100 ns pulse duration, and 5 kHz frequency was used for the machining process. The depth of focus and spot size of the PL were 400 μm and 65 μm , respectively. Figure 4a shows the focal offset distance used for the machining process in this study. While the PL operates within the depth of focus, it ablates material acting like a machining process. In this work, the PL power and scanning speed were fixed at 100 W and 30 m/min, respectively, while varying the travel speed, the input energy density was changed for different experiments. The experimental design presented in Table 3 was constructed to obtain the optimal process parameters for roughness and material removed by the machining process. While the laser power and scan speed were kept constant, the travel speed was varied from 150 mm/min to 375 mm/min with 75 mm/min increments. Since the low input energy density was used during polishing, the number of machining cycles was also varied in the experimental design. The first and third machining cycles traveled along the X-axis while for the second and fourth cycles, the direction was set to travel along the Y-axis. Among 44 deposited samples, the first 12 samples were used to obtain the optimal machining process parameters for surface roughness and material removal determination.

Figure 3b demonstrates the top surface texture of samples #1 to #12 after machining with different process parameters. Samples (#1, #4, #7, and #10) were machined for 1 cycle only with comparatively low input energy density. Therefore, the initial deposition hatching pattern remains visible even after machining. The rest of the samples machined for 2 or 4 cycles depict the hatching pattern due to the machining process as we can see the pattern in both directions.

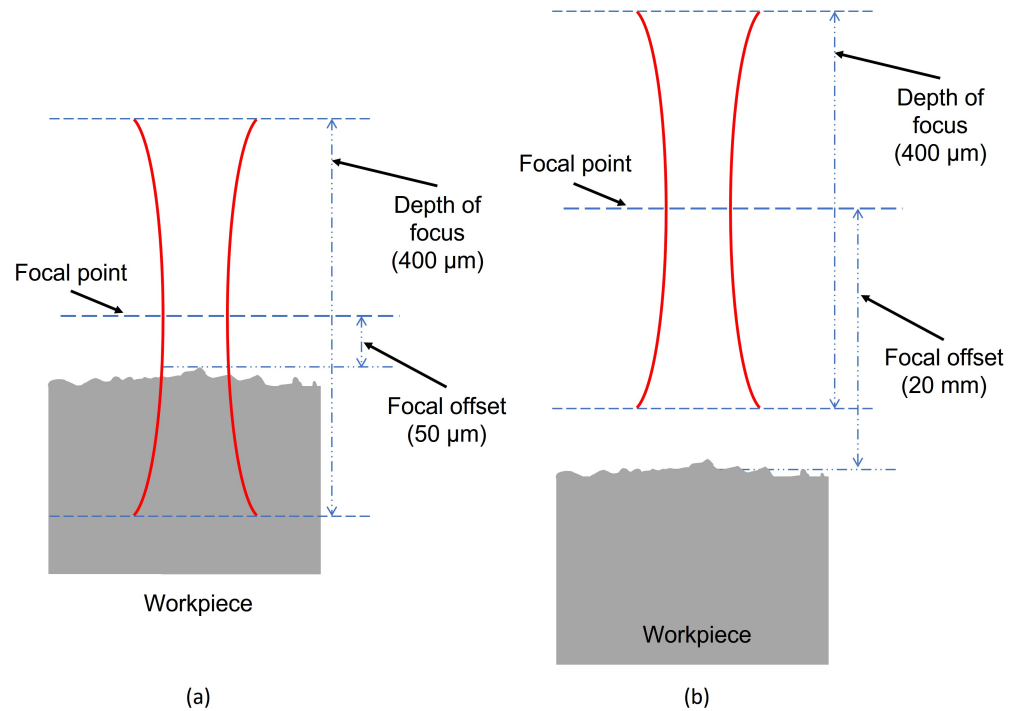


Figure 4. Schematic representation of the pulsed laser focal offset distance used for (a) machining and (b) micro-polishing.

Table 3. Design of experiments for the machining process of Scalmalloy samples #1 to #12.

Sample No.	1	2	3	4	5	6	7	8	9	10	11	12
Travel speed (mm/min)	150	150	150	225	225	225	300	300	300	375	375	375
Number of cycles	1	2	4	1	2	4	1	2	4	1	2	4
Number of scan passes per mm	72	144	288	48	96	192	36	72	144	29	58	116

2.2.4. Polishing

Macro-polishing: Based on the previous study conducted by Ramos et al. [49] while investigating the effect of shallow surface melting and surface over-melting during laser polishing, the process can be classified into two main categories, termed macro-polishing and micro-polishing. The difference between these two categories is primarily defined by the depth of the molten layer, which could be either “deep” or “shallow” with respect to the height of the asperities. The macro-polishing process can be used to polish the surface roughly, while micro-polishing can smooth the roughly polished surface. For the macro-polishing process in this study, the CW laser was used. During the polishing process, the CW laser power was varied from 1000 W to 1600 W with 200 W increments and the travel speed was varied from 300 to 750 mm/min. While the focal offset distance of the CW laser and scan pattern for the macro-polishing process remained identical to the deposition offset distance and scan pattern, unlike the scanning deposition direction, the surface was scanned along the Y-axis during macro-polishing. Table 4 represents different process parameters used for rough polishing the top surface of samples #13 to #28. Before the polishing process, the samples were deposited and machined with optimal process

parameters obtained from the laser-aided machining process. After macro-polishing, the surface roughness of each sample was measured and the optimal process parameters for the macro-polishing process were derived by analyzing the results.

Table 4. Different process parameters used for the macro-polishing of samples #13 to #28.

Sample No.	13	14	15	16	17	18	19	20	21	22	23	24	25	26	27	28
Travel speed (mm/min)	300	300	300	300	450	450	450	450	600	600	600	600	750	750	750	750
CW laser power (W)	1000	1200	1400	1600	1000	1200	1400	1600	1000	1200	1400	1600	1000	1200	1400	1600

Micro-polishing: After obtaining the optimized process parameters for the machining and macro-polishing processes, samples #29 to #44 were deposited, machined, and roughly polished with the resultant process parameters to prepare the samples for further polishing processes. An additional surface finishing process named micro-polishing was introduced in this study to fine finish the surface of the roughly finished part. The PL and scan pattern (shown in Figure 2b) implemented in the machining process were also used for the micro-polishing process. Compared to the machining process, the travel speed, laser power, and focal offset distance were varied. While the scanning speed was equal to the speed used for the machining process, during micro-polishing, the focal offset distance of the PL was set at 20 mm as shown in Figure 4b. The PL power was varied from 40 to 100 W with a 20 W increment and the travel speed was changed from 300 to 750 mm/min with 150 mm/min increments in each step. Table 5 represents different process parameters used for the micro-polishing process. After the final polishing process, the surface roughness of the samples was measured to obtain the optimal process parameters for the micro-polishing process. Figure 5a,b exhibit the surface texture of samples after the final polishing process.

Table 5. Different process parameters used for the micro-polishing of samples #29 to #44.

Sample No.	29	30	31	32	33	34	35	36	37	38	39	40	41	42	43	44
Travel speed (mm/min)	300	300	300	300	450	450	450	450	600	600	600	600	750	750	750	750
Pulsed laser power (W)	40	60	80	100	40	60	80	100	40	60	80	100	40	60	80	100

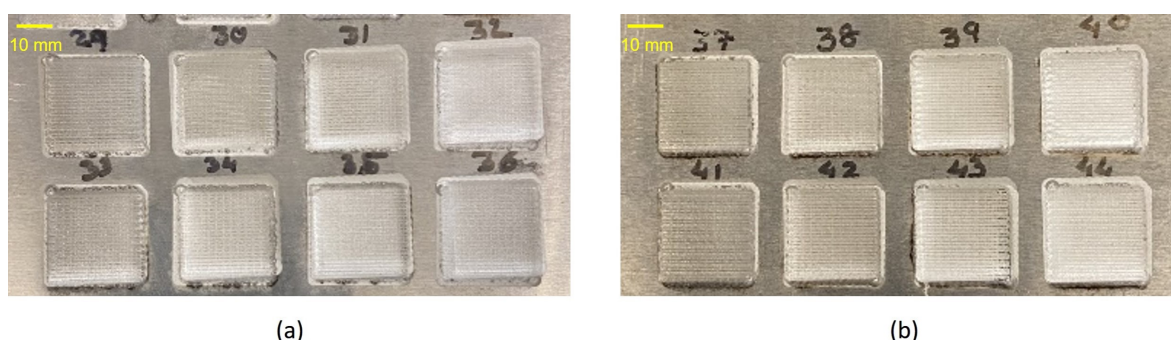


Figure 5. Surface texture of samples (a) #29 to #36 and (b) #37 to #44 after the micro-polishing process.

2.3. Surface Roughness Measurement

In this study, a high-speed non-contact laser displacement sensor (Keyence LK-H052) with 0.025 μm repeatability and 50 μm spot size was used for surface scanning to determine the roughness of the as-built samples and materials removed after the machining process. The as-built samples had a very high roughness as shown in Figure 3a and measuring the

roughness using a surface profilometer might have damaged the touch probe. Therefore, a laser displacement sensor was employed. To scan the surface of the samples, the laser displacement sensor was mounted on the tool holder of a CNC milling machine. A point on the surface of the substrate was fixed as the reference point for scanning the surface both before and after the machining process. A CNC program for raster patterns with 50 μm increments was written to automate the scanning process. The data acquisition rate for the sensor and the scan speed for the motion table were set at 1000 samples/s and 1.25 mm/s, respectively.

The common practice of laser line scanning is along one direction only. The average of the roughness remains the same regardless of the scanning direction. In this study, the as-built samples were scanned along the Y-axis of the deposition. Later, the data were processed to determine the surface roughness. The average roughness (R_a) was calculated according to the ASME B46.1 standard using the following Equation (4),

$$R_a = \frac{1}{n} \sum_{i=1}^n |Z_i - Z_{mean}| \quad (4)$$

where n , i , and Z are the number of total data points, the data number, and the height measured, respectively. We also scanned a few surfaces along the X-axis and compared them with the results obtained from the Y-axis scan. No significant difference was observed since Equation (4) uses millions of scan points and averaging them yields no significant difference. In this study, the laser scanning process was used for the as-built and machined surfaces while a surface profilometer (Mitutoyo SurfTest-212) was utilized to measure the surface roughness after the macro-polishing and micro-polishing processes.

3. Results and Discussion

The LAMP process is a three-step surface treatment method. Machining, macro-polishing, and micro-polishing together can yield a surface with significantly low roughness. While machining ablates some materials from the top surface to minimize high-wavelength surface features (waviness), macro-polishing and micro-polishing can perform the rough and fine polishing of the surface, respectively. During the machining process with different process parameters, this is very important to determine the materials ablated due to laser-aided machining. In this study, the PL power was kept constant to maintain a consistent Gaussian beam profile for the laser while the travel speed and number of cycles were varied according to the design of experiments. Figure 6a shows the average material removed at different machining cycles with varying travel speed.

It is obvious that the average material removed in the laser-aided machining process decreases exponentially with the travel speed at different machining cycles, while the average material removed increases linearly with the number of cycles at different travel speeds (shown in Figure 6b). Therefore, the average material removed can be expressed as Equation (5),

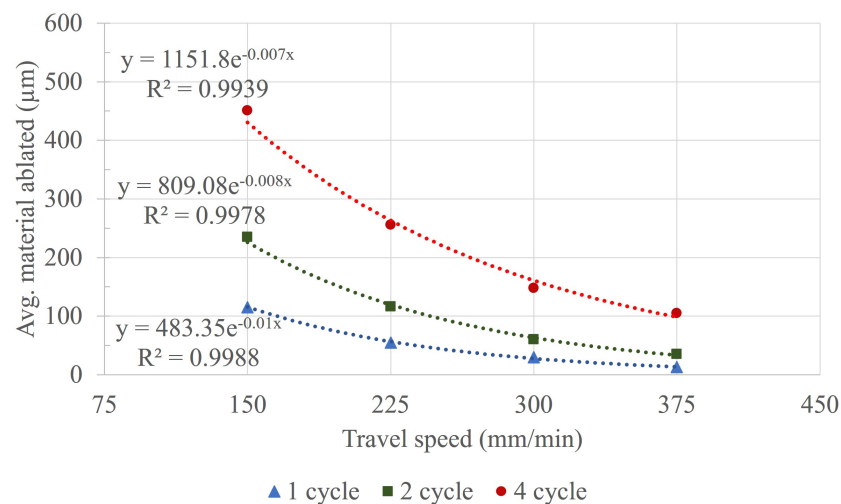
$$R_m = K \times N^\alpha \times e^{-\beta S} \quad (5)$$

where R_m , N , and S are the average material removed, number of machining cycles, and travel speed of the motion table, respectively, while K , α , and β are the coefficients assumed to be dependent on the material and laser properties. To determine the values of the coefficients in Equation (5) and predict the material removed based on the number of machining cycles and travel speed, a multiple linear regression analysis was performed on Equation (6) using the experimental results. A significant regression (Equation (7)) was found with ($F(2, 9) = 308.537, p < 5.12 \times 10^{-9}$) and $R^2 = 0.986$. It is evident that both the number of machining cycles and travel speed were significant to predict the material removed in the laser-aided machining process.

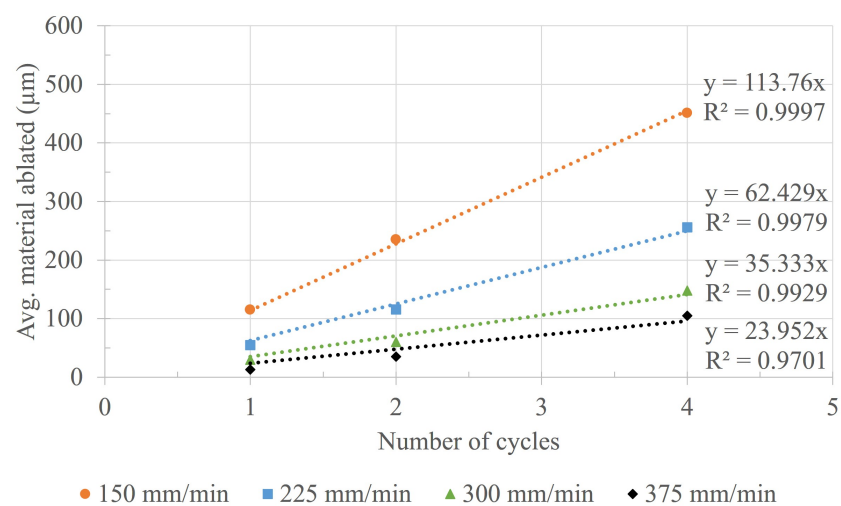
$$\ln R_m = K + \alpha \ln N + \beta \ln S \quad (6)$$

$$R_m = 0.927 \times N^{1.188} \times e^{-0.00365} \tag{7}$$

The powder-fed DED parts initially exhibited a high surface roughness due to both the high- and low-wavelength surface characteristics. The surface roughness (R_a) of all the as-built samples in this study was more than 40 μm on average. The machining process reduces the surface roughness by ablating some materials from the top surface and minimizes the waviness. Figure 7 shows the surface roughness of the samples machined at different travel speeds with varying numbers of cycles. While the 4-cycle machining ablates a comparatively consistent amount of material following the mathematical model, the surface roughness increases when compared with the roughness achieved with 2 cycles. In conventional polishing processes, achieving an optimal roughness, over-polishing increases the roughness of the surface instead of decreasing it. When a material is overly polished by an abrasive material, the polishing process creates additional peaks and valleys on the surface worsening the surface quality. In laser-aided machining, repetitive laser melting or ablation may also create additional peaks and valleys due to the surface tension associated with the temperature gradient of repetitive laser remelting.



(a)



(b)

Figure 6. Average materials removed due to machining process at (a) different travel speeds and (b) machining cycles.

The objective of these experiments was to determine the machining process parameters with minimal material removal but maximum surface roughness reduction. No significant

surface roughness reduction was observed at the highest speed (375 mm/min) for the unit machining cycle, although as the speed decreases, the roughness reduction increases. This is because the input energy density increases with the decreasing speed. The effect of the number of machining cycles shows that 2-cycle machining (in both X and Y directions) exhibits improved surface quality at different speeds than 4-cycle machining. Additionally, 2-cycle machining ablates fewer materials than 4-cycle machining. Therefore, 2-cycle machining at a 300 mm/min speed was chosen as the optimized machining process. Later, these parameters were used to machine samples #13 to #44.

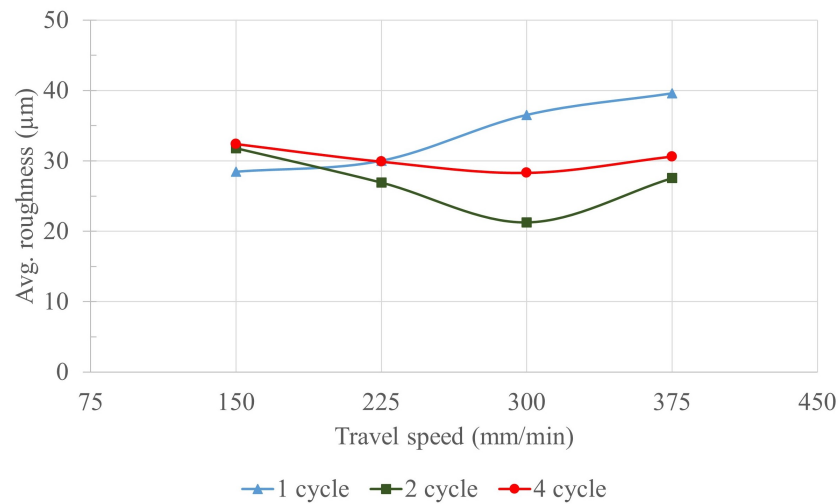


Figure 7. Average surface roughness of samples #1 to #12 after machining process. The PL power, focal offset distance, and scan speed were 100 W, 50 µm, and 30 m/min, respectively.

After machining, a reduction in surface roughness was observed. To further improve the surface quality, macro-polishing was performed using the CW laser at different powers and travel speeds. The surface roughness of samples #13 to #28 is shown in Figure 8. At all different laser powers, the surface roughness was reduced but a more than 90% reduction in roughness between machining and macro-polishing processes was observed between 450 and 600 mm/min speeds and 1200 W laser power. Therefore, 500 mm/min travel speed and 1200 W power were selected as the optimized process parameters for the macro-polishing process.

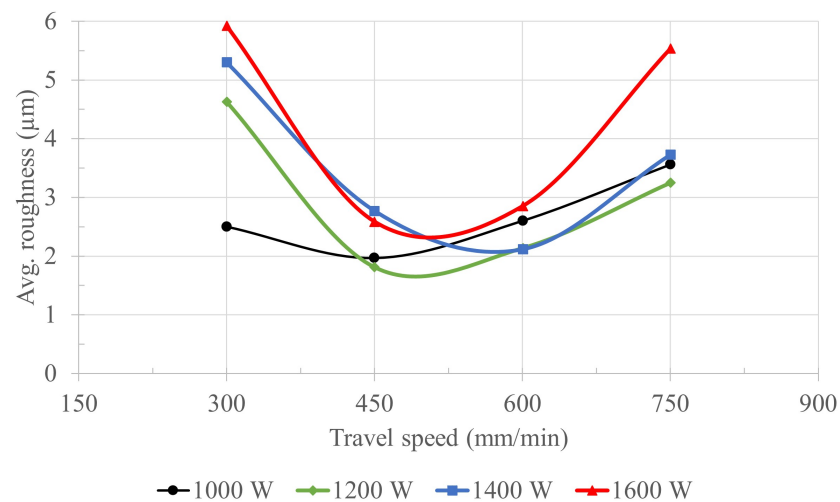


Figure 8. Average surface roughness of samples #13 to #28 after macro-polishing process.

While macro-polishing reduces the surface roughness mostly in the entire LAMP process, the micro-polishing process was implemented in this study for further smoothing the surface quality after the macro-polishing process. Figure 9 illustrates the roughness after micro-polishing the samples with different process parameters. Prior to implementing this process, all the samples were machined and macro-polished using the optimized parameters determined in this study. Increasing the scanning speed during fine polishing of the surface did not help substantially in improving the surface quality since the laser could not originate a significant melt pool to polish the surface at higher speeds. As the PL power increased, no significant improvement in surface quality was observed because increasing the laser power increases the melt pool depth and as a result creates additional roughness due to high energy input. A reduction in surface roughness was seen only for 40 W PL power at all different speeds but the travel speed of 300 mm/min showed the highest improvement in surface quality. However, the parameters for sample #29 showed a nominal surface quality improvement within the boundary of the experimental design, The band of the process parameters chosen in this study does not confine the lower boundary of the parameters for optimal surface quality. As a future study, a new experimental design covering a wide range of PL powers and higher scan speeds can help to obtain optimized process parameters for improved surface quality.

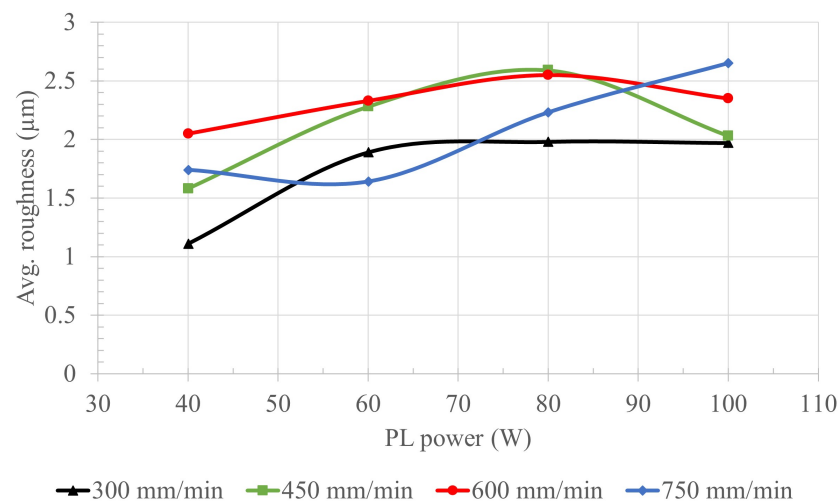


Figure 9. Average surface roughness of samples #29 to #44 after the micro-polishing process. The PL focal offset distance and scan speed were 50 mm and 30 m/min, respectively.

For further investigation, to demonstrate the effectiveness of machining prior to polishing, an additional sample was deposited and polished with optimized parameters without machining. Figure 10a–c illustrate the line-scanned surface profile of the as-built, LAMP processed, and polished sample. The as-built sample surface (shown in Figure 10a) shows both high and low waviness in surface topography while the LAMP processed surface in Figure 10b demonstrates the least waviness compared to the polished surface illustrated in Figure 10c. Therefore, the LAMP process (combination of laser-aided machining, macro-polishing, and micro-polishing) can be an effective method for improving the surface quality of AM metals due to minimizing the surface waviness and roughness and achieving an overall surface quality improvement of more than 97% when compared to the as-built part.

Due to the limitation in the degree of freedom of the CNC motion table, in this study, the LAMP process was applied only on the XY (horizontal) plane of the deposited materials. However, a five-axis machine or a robotic AM system can facilitate the process with the advantage of machining and polishing at different planes as well.

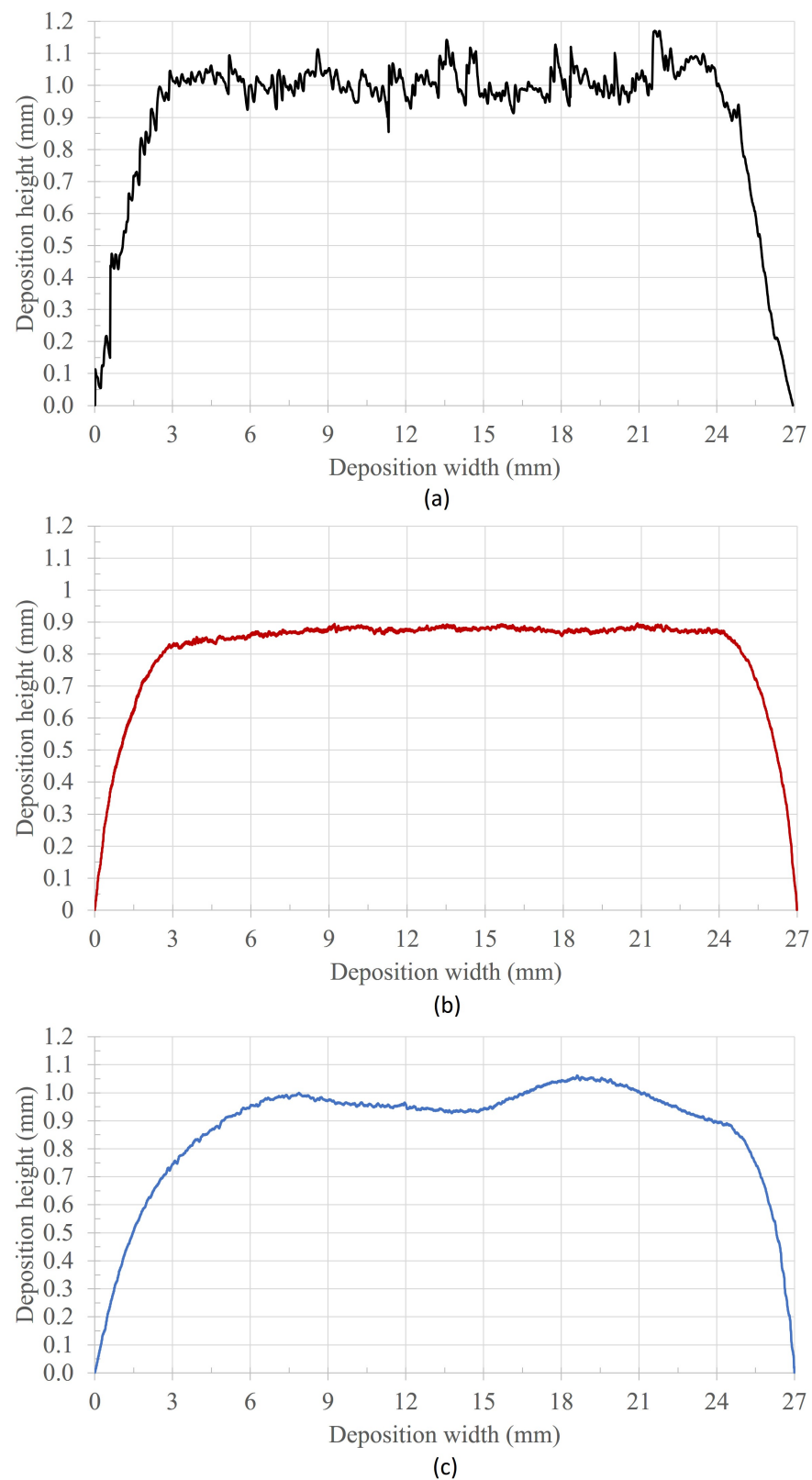


Figure 10. Surface profile (scanned line along Y axis) of (a) as-built sample, (b) sample machined and polished with optimized process parameters, and (c) sample not machined but polished with optimized process parameters.

4. Conclusions

AM metal parts exhibit a high surface roughness. To improve the surface quality of AM materials, post-processing is required. In this paper, we proposed a laser-aided machining and polishing process to reduce the surface roughness of AM metals. The conclusions of this research work can be summarized as follows.

- In this study, multiple lasers were integrated for fabrication, machining, and polishing of AM materials in the same build chamber. A unique scan pattern was also introduced to implement low energy input for machining and polishing of metals. A two-step polishing process using CW and pulsed laser was employed for rough and fine polishing.
- A systematic approach was discussed and implemented to obtain optimal process parameters for machining and polishing of AM aluminum alloy. A regression analysis was performed, and a mathematical model was derived from the experimental results to predict the material removed during the machining process.
- The roughness and waviness in the surface topography were minimized using the combined machining and polishing process and a more than 97% improvement in surface quality was achieved.

Future works may include implementing the process to obtain geometric dimensions and tolerances (GD&T) for custom parts, applying the method for other AM processes, materials, and alloys. The influence of the laser-aided machining and polishing process on the microstructure and mechanical properties such as hardness, corrosion resistance, and fatigue performance can also be a part of future studies.

Author Contributions: The contribution of each author is summarized as conceptualization, M.M.P., S.P. and S.P.I.; methodology, M.M.P. and S.P.; software, M.M.P.; data curation, S.P.; validation M.M.P.; formal analysis, M.M.P. and S.P.; investigation, M.M.P. and S.P.; writing—original draft, M.M.P.; writing—review and editing, M.M.P., S.P.I. and F.L.; visualization, M.M.P.; supervision, S.P.I. and F.L.; project administration, S.P.I. and F.L.; funding acquisition, S.P.I. and F.L. All authors have read and agreed to the published version of the manuscript.

Funding: This research was supported by National Science Foundation Grants CMMI-1625736 and EEC 1937128. Part of the work was also funded by the Department of Energy's Kansas City National Security Campus, which is operated and managed by Honeywell Federal Manufacturing Technologies, LLC, under contract number DE-NA0002839, the Intelligent Systems Center, and the Material Research Center at Missouri University of Science and Technology. Their support is greatly appreciated.

Conflicts of Interest: The authors declare no conflict of interest.

References

1. Zhang, Y.; Wu, L.; Guo, X.; Kane, S.; Deng, Y.; Jung, Y.G.; Lee, J.H.; Zhang, J. Additive manufacturing of metallic materials: A review. *J. Mater. Eng. Perform.* **2018**, *27*, 1–13. [\[CrossRef\]](#)
2. Frazier, W.E. Metal additive manufacturing: A review. *J. Mater. Eng. Perform.* **2014**, *23*, 1917–1928. [\[CrossRef\]](#)
3. Lewandowski, J.J.; Seifi, M. Metal additive manufacturing: A review of mechanical properties. *Annu. Rev. Mater. Res.* **2016**, *46*, 151–186. [\[CrossRef\]](#)
4. Gibson, I.; Rosen, D.; Stucker, B.; Khorasani, M. Design for additive manufacturing. In *Additive Manufacturing Technologies*; Springer: Berlin/Heidelberg, Germany, 2021; pp. 555–607.
5. Wong, K.V.; Hernandez, A. A review of additive manufacturing. *Int. Sch. Res. Not.* **2012**, *2012*, 208760. [\[CrossRef\]](#)
6. Parvez, M.; Chen, Y.; Newkirk, J.; Liou, F. Comparison of fatigue performance between additively manufactured and wrought 304L stainless steel using a novel fatigue test setup. In Proceedings of the Solid Freeform Fabrication, Austin, TX, USA, 12–14 August 2019; pp. 353–363.
7. Ramos-Grez, J.; Bourell, D. Reducing surface roughness of metallic freeform-fabricated parts using non-tactile finishing methods. *Int. J. Mater. Prod. Technol.* **2004**, *21*, 297–316. [\[CrossRef\]](#)
8. Abele, E.; Kniepkamp, M. Analysis and optimisation of vertical surface roughness in micro selective laser melting. *Surf. Topogr. Metrol. Prop.* **2015**, *3*, 034007. [\[CrossRef\]](#)
9. Calignano, F.; Manfredi, D.; Ambrosio, E.; Iuliano, L.; Fino, P. Influence of process parameters on surface roughness of aluminum parts produced by DMLS. *Int. J. Adv. Manuf. Technol.* **2013**, *67*, 2743–2751. [\[CrossRef\]](#)

10. Parvez, M.M.; Pan, T.; Chen, Y.; Karnati, S.; Newkirk, J.W.; Liou, F. High Cycle Fatigue Performance of LPBF 304L Stainless Steel at Nominal and Optimized Parameters. *Materials* **2020**, *13*, 1591. [[CrossRef](#)]
11. Mills, K.; Keene, B.; Brooks, R.; Shirali, A. Marangoni effects in welding. *Philos. Trans. R. Soc. Lond. Ser. A Math. Phys. Eng. Sci.* **1998**, *356*, 911–925. [[CrossRef](#)]
12. Cho, M.H.; Farson, D.F. Understanding bead hump formation in gas metal arc welding using a numerical simulation. *Metall. Mater. Trans. B* **2007**, *38*, 305–319. [[CrossRef](#)]
13. Hauser, C.; Childs, T.; Dalgamo, K. Selective laser sintering of stainless steel 314S HC processed using room temperature powder beds. In Proceedings of the Solid Freeform Fabrication, Austin, TX, USA, 11–13 August 1999.
14. Klocke, F.; Wagner, C. Coalescence behaviour of two metallic particles as base mechanism of selective laser sintering. *CIRP Ann.* **2003**, *52*, 177–180. [[CrossRef](#)]
15. Li, R.; Liu, J.; Shi, Y.; Wang, L.; Jiang, W. Balling behavior of stainless steel and nickel powder during selective laser melting process. *Int. J. Adv. Manuf. Technol.* **2012**, *59*, 1025–1035. [[CrossRef](#)]
16. Kruth, J.P.; Vandenbroucke, B.; Van Vaerenbergh, J.; Mercelis, P. Benchmarking of different SLS/SLM processes as rapid manufacturing techniques. In Proceedings of the International Conference Polymers & Moulds Innovations PMI 2005, Gent, Belgium, 20–23 April 2005.
17. Mumtaz, K.; Hopkinson, N. Top surface and side roughness of Inconel 625 parts processed using selective laser melting. *Rapid Prototyp. J.* **2009**, *15*, 96–103. [[CrossRef](#)]
18. Strano, G.; Hao, L.; Everson, R.M.; Evans, K.E. Surface roughness analysis, modelling and prediction in selective laser melting. *J. Mater. Process. Technol.* **2013**, *213*, 589–597. [[CrossRef](#)]
19. Vilar, R.M. Laser cladding. In Proceedings of the ALT'02 International Conference on Advanced Laser Technologies. International Society for Optics and Photonics, Adelboden, Switzerland, 16–20 September 2002; Volume 5147, pp. 385–392.
20. Parvez, M.M.; Chen, Y.; Karnati, S.; Coward, C.; Newkirk, J.W.; Liou, F. A Displacement Controlled Fatigue Test Method for Additively Manufactured Materials. *Appl. Sci.* **2019**, *9*, 3226. [[CrossRef](#)]
21. Spierings, A.B.; Starr, T.L.; Wegener, K. Fatigue performance of additive manufactured metallic parts. *Rapid Prototyp. J.* **2013**, *19*, 88–94. [[CrossRef](#)]
22. Taminger, K.; Hafley, R.A.; Fahringer, D.T.; Martin, R.E. Effect of surface treatments on electron beam freeform fabricated aluminum structures. In Proceedings of the Solid Freeform Fabrication, Austin, TX, USA, 11–13 August 2004.
23. Löber, L.; Flache, C.; Petters, R.; Kühn, U.; Eckert, J. Comparison of different post processing technologies for SLM generated 316L steel parts. *Rapid Prototyp. J.* **2013**, *19*, 173–179. [[CrossRef](#)]
24. Beaucamp, A.T.; Namba, Y.; Charlton, P.; Jain, S.; Graziano, A.A. Finishing of additively manufactured titanium alloy by shape adaptive grinding (SAG). *Surf. Topogr. Metrol. Prop.* **2015**, *3*, 024001. [[CrossRef](#)]
25. Flynn, J.M.; Shokrani, A.; Newman, S.T.; Dhokia, V. Hybrid additive and subtractive machine tools—Research and industrial developments. *Int. J. Mach. Tools Manuf.* **2016**, *101*, 79–101. [[CrossRef](#)]
26. Ermergen, T.; Taylan, F. Review on Surface Quality Improvement of Additively Manufactured Metals by Laser Polishing. *Arab. J. Sci. Eng.* **2021**, *46*, 7125–7141. [[CrossRef](#)]
27. Krishnan, A.; Fang, F. Review on mechanism and process of surface polishing using lasers. *Front. Mech. Eng.* **2019**, *14*, 299–319. [[CrossRef](#)]
28. Deng, T.; Li, J.; Zheng, Z. Fundamental aspects and recent developments in metal surface polishing with energy beam irradiation. *Int. J. Mach. Tools Manuf.* **2020**, *148*, 103472. [[CrossRef](#)]
29. Giorleo, L.; Ceretti, E.; Giardini, C. Ti surface laser polishing: Effect of laser path and assist gas. *Procedia Cirp* **2015**, *33*, 446–451. [[CrossRef](#)]
30. Bordatchev, E.V.; Hafiz, A.M.; Tutunea-Fatan, O.R. Performance of laser polishing in finishing of metallic surfaces. *Int. J. Adv. Manuf. Technol.* **2014**, *73*, 35–52. [[CrossRef](#)]
31. Mohajerani, S.; Bordatchev, E.V.; Tutunea-Fatan, O.R. Recent developments in modeling of laser polishing of metallic materials. *Lasers Manuf. Mater. Process.* **2018**, *5*, 395–429. [[CrossRef](#)]
32. Marimuthu, S.; Triantaphyllou, A.; Antar, M.; Wimpenny, D.; Morton, H.; Beard, M. Laser polishing of selective laser melted components. *Int. J. Mach. Tools Manuf.* **2015**, *95*, 97–104. [[CrossRef](#)]
33. Liang, C.; Hu, Y.; Liu, N.; Zou, X.; Wang, H.; Zhang, X.; Fu, Y.; Hu, J. Laser polishing of Ti6Al4V fabricated by selective laser melting. *Metals* **2020**, *10*, 191. [[CrossRef](#)]
34. Lee, S.; Ahmadi, Z.; Pegues, J.W.; Mahjouri-Samani, M.; Shamsaei, N. Laser polishing for improving fatigue performance of additive manufactured Ti-6Al-4V parts. *Opt. Laser Technol.* **2021**, *134*, 106639. [[CrossRef](#)]
35. Willenborg, E. Polishing with laser radiation. *Kunststoffe Int.* **2007**, *97*, 37.
36. Perry, T.L.; Werschmoeller, D.; Li, X.; Pfefferkorn, F.E.; Duffie, N.A. Micromelting for laser micro polishing of meso/micro metallic components. In Proceedings of the International Manufacturing Science and Engineering Conference, Atlanta, GA, USA, 15–18 October 2007; Volume 42908, pp. 363–369.
37. Wang, H.Y.; Bourell, D.; Beaman, J. Laser polishing of silica slotted rods. *Mater. Sci. Technol.* **2003**, *19*, 382–387. [[CrossRef](#)]
38. Mohajerani, S.; Miller, J.D.; Tutunea-Fatan, O.R.; Bordatchev, E.V. Thermo-physical modelling of track width during laser polishing of H13 tool steel. *Procedia Manuf.* **2017**, *10*, 708–719. [[CrossRef](#)]

39. Vatsya, S.; Nikumb, S. Modeling of fluid dynamical processes during pulsed-laser texturing of material surfaces. *Phys. Rev. B* **2003**, *68*, 035410. [[CrossRef](#)]
40. Gora, W.S.; Tian, Y.; Cabo, A.P.; Ardron, M.; Maier, R.R.; Prangnell, P.; Weston, N.J.; Hand, D.P. Enhancing surface finish of additively manufactured titanium and cobalt chrome elements using laser based finishing. *Phys. Procedia* **2016**, *83*, 258–263. [[CrossRef](#)]
41. Ćwikła, M.; Dziejczak, R.; Reiner, J. Influence of Overlap on Surface Quality in the Laser Polishing of 3D Printed Inconel 718 under the Effect of Air and Argon. *Materials* **2021**, *14*, 1479. [[CrossRef](#)]
42. Zhang, D.; Yu, J.; Li, H.; Zhou, X.; Song, C.; Zhang, C.; Shen, S.; Liu, L.; Dai, C. Investigation of laser polishing of four selective laser melting alloy samples. *Appl. Sci.* **2020**, *10*, 760. [[CrossRef](#)]
43. Lambarri, J.; Leunda, J.; Soriano, C.; Sanz, C. Laser surface smoothing of nickel-based superalloys. *Phys. Procedia* **2013**, *41*, 255–265. [[CrossRef](#)]
44. Chen, L.; Zhang, X. Modification the surface quality and mechanical properties by laser polishing of Al/PLA part manufactured by fused deposition modeling. *Appl. Surf. Sci.* **2019**, *492*, 765–775. [[CrossRef](#)]
45. Ma, C.; Vadali, M.; Duffie, N.A.; Pfefferkorn, F.E.; Li, X. Melt pool flow and surface evolution during pulsed laser micro polishing of Ti6Al4V. *J. Manuf. Sci. Eng.* **2013**, *135*, 061023. [[CrossRef](#)]
46. Miller, J.D.; Tutunea-Fatan, O.R.; Bordatchev, E.V. Experimental analysis of laser and scanner control parameters during laser polishing of H13 steel. *Procedia Manuf.* **2017**, *10*, 720–729. [[CrossRef](#)]
47. Chow, M.T.; Bordatchev, E.V.; Knopf, G.K. Experimental study on the effect of varying focal offset distance on laser micropolished surfaces. *Int. J. Adv. Manuf. Technol.* **2013**, *67*, 2607–2617. [[CrossRef](#)]
48. Perry, T.L.; Werschmoeller, D.; Li, X.; Pfefferkorn, F.E.; Duffie, N.A. The effect of laser pulse duration and feed rate on pulsed laser polishing of microfabricated nickel samples. *J. Manuf. Sci. Eng.* **2009**, *131*. [[CrossRef](#)]
49. Ramos, J.; Bourell, D.; Beaman, J. Surface over-melt during laser polishing of indirect-SLS metal parts. *MRS Online Proc. Libr. (OPL)* **2002**, 758. [[CrossRef](#)]
50. Schneider, C.W.; Lippert, T. Laser ablation and thin film deposition. In *Laser Processing of Materials*; Springer: Berlin/Heidelberg, Germany, 2010; pp. 89–112.
51. Brown, M.S.; Arnold, C.B. Fundamentals of laser-material interaction and application to multiscale surface modification. In *Laser Precision Microfabrication*; Springer: Berlin/Heidelberg, Germany, 2010; pp. 91–120.
52. Rosa, B.; Hascoet, J.Y.; Mognol, P. Modeling and optimization of laser polishing process. In *Applied Mechanics and Materials*; Trans Tech Publ.: Freienbach, Switzerland, 2014; Volume 575, pp. 766–770.
53. Chen, C.; Tsai, H.L. Fundamental study of the bulge structure generated in laser polishing process. *Opt. Lasers Eng.* **2018**, *107*, 54–61. [[CrossRef](#)]
54. Yung, K.; Xiao, T.; Choy, H.; Wang, W.; Cai, Z. Laser polishing of additive manufactured CoCr alloy components with complex surface geometry. *J. Mater. Process. Technol.* **2018**, *262*, 53–64. [[CrossRef](#)]
55. Kumstel, J.; Kirsch, B. Polishing titanium-and nickel-based alloys using cw-laser radiation. *Phys. Procedia* **2013**, *41*, 362–371. [[CrossRef](#)]
56. Dai, W.; Li, J.; Zhang, W.; Zheng, Z. Evaluation of fluences and surface characteristics in laser polishing SKD 11 tool steel. *J. Mater. Process. Technol.* **2019**, *273*, 116241. [[CrossRef](#)]
57. dos Santos Solheid, J.; Seifert, H.J.; Pflöging, W. Laser surface modification and polishing of additive manufactured metallic parts. *Procedia Cirp* **2018**, *74*, 280–284. [[CrossRef](#)]
58. Nüsser, C.; Sändker, H.; Willenborg, E. Pulsed laser micro polishing of metals using dual-beam technology. *Phys. Procedia* **2013**, *41*, 346–355. [[CrossRef](#)]
59. Caggiano, A.; Teti, R.; Alfieri, V.; Caiazzo, F. Automated Laser Polishing for surface finish enhancement of additive manufactured components for the automotive industry. *Prod. Eng.* **2021**, *15*, 109–117. [[CrossRef](#)]
60. Awd, M.; Tenkamp, J.; Hirtler, M.; Siddique, S.; Bambach, M.; Walther, F. Comparison of microstructure and mechanical properties of Scalmalloy® produced by selective laser melting and laser metal deposition. *Materials* **2018**, *11*, 17. [[CrossRef](#)]
61. Baig, S.; Ghiaasiaan, S.R.; Shamsaei, N. Effect of Heat Treatment on the Microstructure and Mechanical Properties of LB-PBF AlSi10Mg and Scalmalloy. In *Light Metals 2021: 50th Anniversary Edition*; Springer International Publishing: Berlin/Heidelberg, Germany, 2021; pp. 119–125.
62. Cordova, L.; Macia, E.; Campos, M.; Tinga, T. Mechanical properties of aluminum alloys produced by Metal Additive Manufacturing. In *Proceedings of the Euro PM 2018 Congress & Exhibition, Bilbao, Spain, 14–18 October 2018*.
63. Texture, S. *ANSI/ASME B46. 1*; American Society of Mechanical Engineers: New York, NY, USA, 1995; Volume 10017.
64. Ma, C.; Guan, Y.; Zhou, W. Laser polishing of additive manufactured Ti alloys. *Opt. Lasers Eng.* **2017**, *93*, 171–177. [[CrossRef](#)]
65. Bhaduri, D.; Penchev, P.; Batal, A.; Dimov, S.; Soo, S.L.; Sten, S.; Harrysson, U.; Zhang, Z.; Dong, H. Laser polishing of 3D printed mesoscale components. *Appl. Surf. Sci.* **2017**, *405*, 29–46. [[CrossRef](#)]